Institute of Space and Aeronautical Science, University of Tokyo
Report No. 407, November 1966

Combustion Characteristics and Ballistic Performance of Dual-Layer Propellant Grains for End-Burning Type Rocket Motors

By

Akira IWAMA, Shoichiro AOYAGI, Teruo SOFUE
and Kiroku YAMAZAKI

Summary. A laboratory-scale rocket motor of the end-burning type has been used to characterize the combustion aspect and ballistic performance of concentric dual-layer propellant grains. The inner-layer and the outer-layer are polybutadiene~potassium perchlorate-based propellant with comparatively high regression rate and slow burning polyurethane~ammonium perchlorate propellant, respectively. Under the condition of constant outer-layer diameter firing experiments have been carried out varying the inner-layer diameter et al., in order to determine optimum grain design.

Increasing the ratio of the inner-layer to the outer-layer diameter resulted in remarkable increase in the steepness of pressure-time curves. It was noted that there occurred a gutter in the boundary region of these two grain layers at the burning surface where the steady-state combustion was interrupted. An erosive burning effect due to the interaction of turbulent gas flows generating from each burning surface with different regression rates, was postulated as the most likely cause of this phenomenon. By means of one-dimentional transparent midget motor, characteristics of heterogeneous combustion of dual-layer grains containing Al and Al-Mg alloy particles, were discussed and compared with those of simple end-burning grain.

1. INTRODUCTION

Generally, the end-burning motors have simpler geometrical configuration of the propellant grains and higher loading density than the radial-burning type. However, despite these benefits, less interest is being paid toward the end-burning rocket motors because of many problems to be solved. Indeed, there are several disadvantages inherent to this combustion chamber; actually, it is not easy to operate the motors at the high pressure equivalent to the ordinal burning pressure in side-burning rocket motors.

Protection of the hardware from the hot gases for a long thrust duration and reduction of the conductive heat flow along the chamber wall which may cause the unexpected side-surface ignition and deflagration, are indispensable. Consequently, it is necessary to develop the heat insulator of the high quality as the lining material for the lateral surface of the grain. However, we have no satisfactory insulator that can potentially contribute to the avoidance of the troubles leading to anomalous

pressure-time history, undesirable and dangerous over-pressures and excess heat transfer.

Defects of the thrust chamber structure are evidently associated with the nature that the charged grain is pressed against the fore-head direction by the gaseous products. Accordingly, the intermission between grain periphery and restrictor or heat insulator might happen, if the great care on the loading procedure is not taken, but too thick insulator would result in sacrificing over-all performance because of the diminution of the propellant grain amount.

Furthermore, there are several serious requirements for the ballistic performance of the end-burning grains; fast burning rate as well as high specific impulse are needed for a sufficient acceleration for launching the vehicle and flight at comparatively low altitude. It is also required that pressure index of the regression rate is small as far as possible, in order to obtain smooth combustion regardless of the chamber pressure.

Unfortunately, these requirements have not satisfactorily been realized on the level of the current composite propellants. Fast burning propellant has generally high pressure index of the regression rate. It means that response of this propulsion system is sensitive to a disturbance capable of triggering unstable combustion.

Consequently, an attempt of making the end-burning grain motor available with some devices on the grain design is of importance. The dual-layer propellant grain method has been used extensively for side-burning motors to generate the optimum thrust [1] [2]. However, its positive application to the end-burning motors has not been undertaken systematically, since the great parts of the current solid rocket motors are occupied by side-burning grain systems.

This report presents the feasibility of the dual-layer propellant grain to overcome the weak points being involved in the end-burning motor, and describes combustion characteristics obtained by nearly fifty firings.

2. Experiments and Discussions

2.1. Dual-Layer Propellant Grain

Grain preparation

The ingredients of the composite propellants used in this study are shown in Table 1. The grain was prepared by the casting method without any adhesive between outer and inner-layer composed of polyurethane and polybutadiene

Table 1. Solid propellant ingredients

Symbol	Inner layer		Outer layer
	A	B	C
Fuel-binder	Polybutadiene 20 (parts by weights)	25	Polyurethane 25
Oxidizer	Potassium perchlorate 80	75	Ammonium perchlorate 75
Metal additive	Al-Mg particles 12	12	Al particles 7
Burning catalyst	Copper chromite 4	4	——

propellant, respectively. First, the blended dough of polyurethane materials, ammonium perchlorate, and aluminium particles was poured into the cylindrical mould whose inside was coated with silicon grease. After the polyurethane propellant cured, the dough composed of polybutadiene materials, potassium perchlorate, copper chromite, and aluminium-magnesium alloy particles was directly poured into the perforated space of polyurethane propellant.

The difficulty of casting operation of the blended-dough which contained large amount of metal and oxidizer more than 82% was resolved only by adjusting the particle size distribution of the oxidizer and the additives. Cured propellant grain was machined in the form of a cylinder of 96 mm in diameter and 80~90 mm in length.

Then, polyurethane elastomer was applied on the lateral surface of the grain as an inhibitor, which had the similar compositions to fuel-binder of the outer-layer and it was charged into the motor case by means of cartridge-bonding. Fig. 1 shows a schematic drawing of the dual-layer grain motor. Here the outer-layer has comparatively slow burning rate with weak dependency on the ambient pressure, whereas the inner-layer is of higher burning rate but has high sensitivity to the combustion pressures.

Characteristics of this grain consist in using Al-Mg alloy particles (Magnarium). "Magnarium" lends itself to the increase of both chemical reactivity and energy content as a metallized propellant. Namely, it can be expected to be more effective for thrust generation than aluminium particle, and thereby higher burning rate is realized.

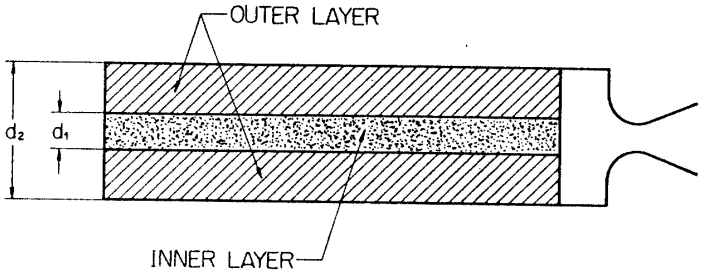

FIG. 1. Schematic drawing of dual-layer grains.

Linear burning rate measured by means of a bomb method

The burning rate measured in a strand-burner with these propellants are shown in Fig. 2. The inner-layer exhibits high pressure index of the burning rate and expresses a striking contrast to the outer one.

Given an expression for the linear burning rate (r) as a function of the ambient pressure (p)

$$r=ap^n \tag{1}$$

, the value of the pressure index (n) is determined from the lines of Fig. 2 as follows:

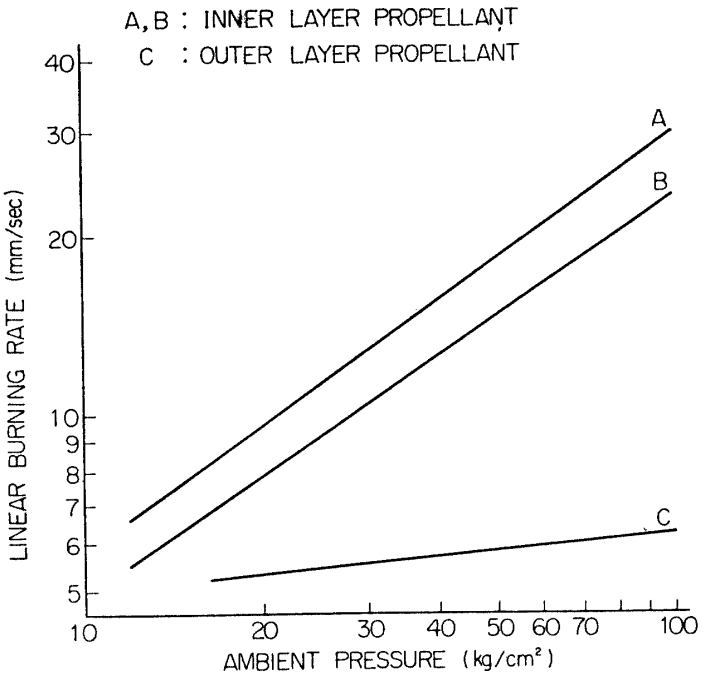

FIG. 2. Relation between ambient pressure and linear burning rate of propellant grain layers, measured by means of bomb method.

Propellant	Pressure index (n)
A	0.69
B	0.67
C	0.10

The high pressure index of the inner-layer propellant suggests that its application to the simple end-burning grain may be difficult to sustain normal combustion at the high pressures, resulting in poor reliability from the view point of the unstable combustion induced by the pressure disturbance. However, it is not considered to be inhibitory property for the use to the dual-layer grain motors, because as a matter of fact, no acoustic unstable combustion has occurred during this study and the burning rate difference increases as the chamber pressure increases, introducing remarkable pressure progressivity.

Static firing tests

By using a midget motor of 100 mm inside diameter, firing experiments were carried out, varying inner-layer propellant diameter, fuel/oxidizer ratio of the inner-layer, and restriction ratio. Fig. 3 shows some examples of the characteristic pressure-time history. Estimates of these pressure progressivity indicate that there are suitable or limiting ratios of the inner-layer diameter to the outer one for a given grain length. The values for them are 0.4~0.7 with L/D ratio of the grain of 0.83.

As L/D increases, the upper limit of the available ratio of the inner-layer to

the outer decreases. Increase in the inner-layer diameter with the outer-layer diameter fixed, corresponds to the increase of steepness of the pressure-time curves. Extremely thin outer-layer would cause erratic motor performance or fracture. It should be noted, however, that the unstable combustion and anomalous over-pressure exceeding the anticipated chamber pressure have not been experi-

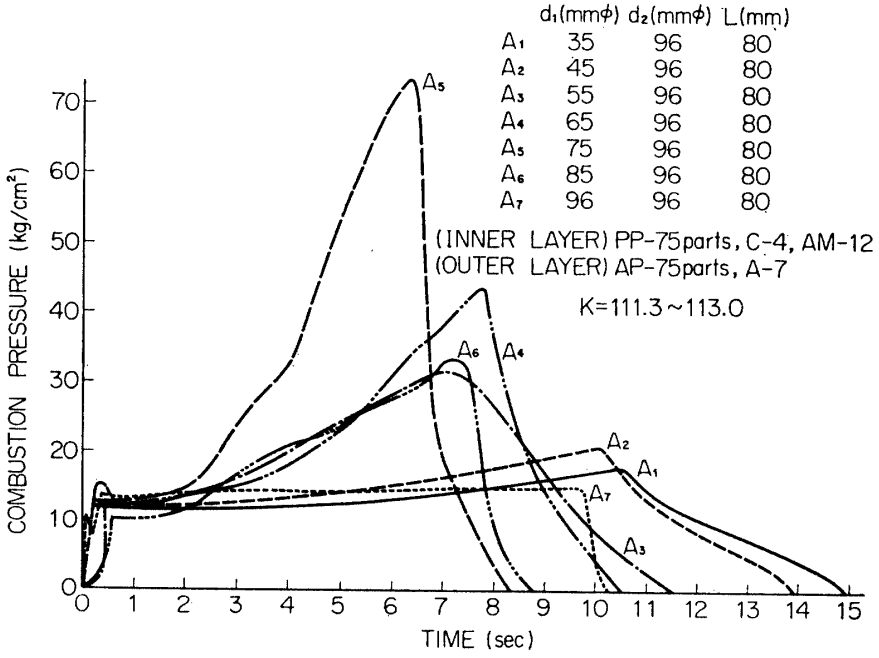

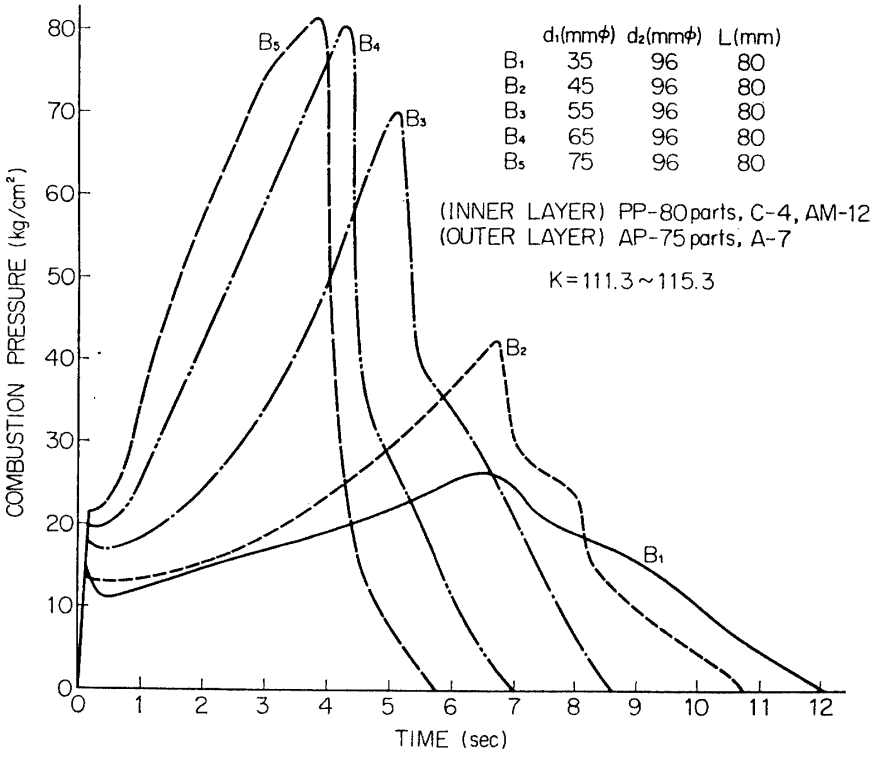

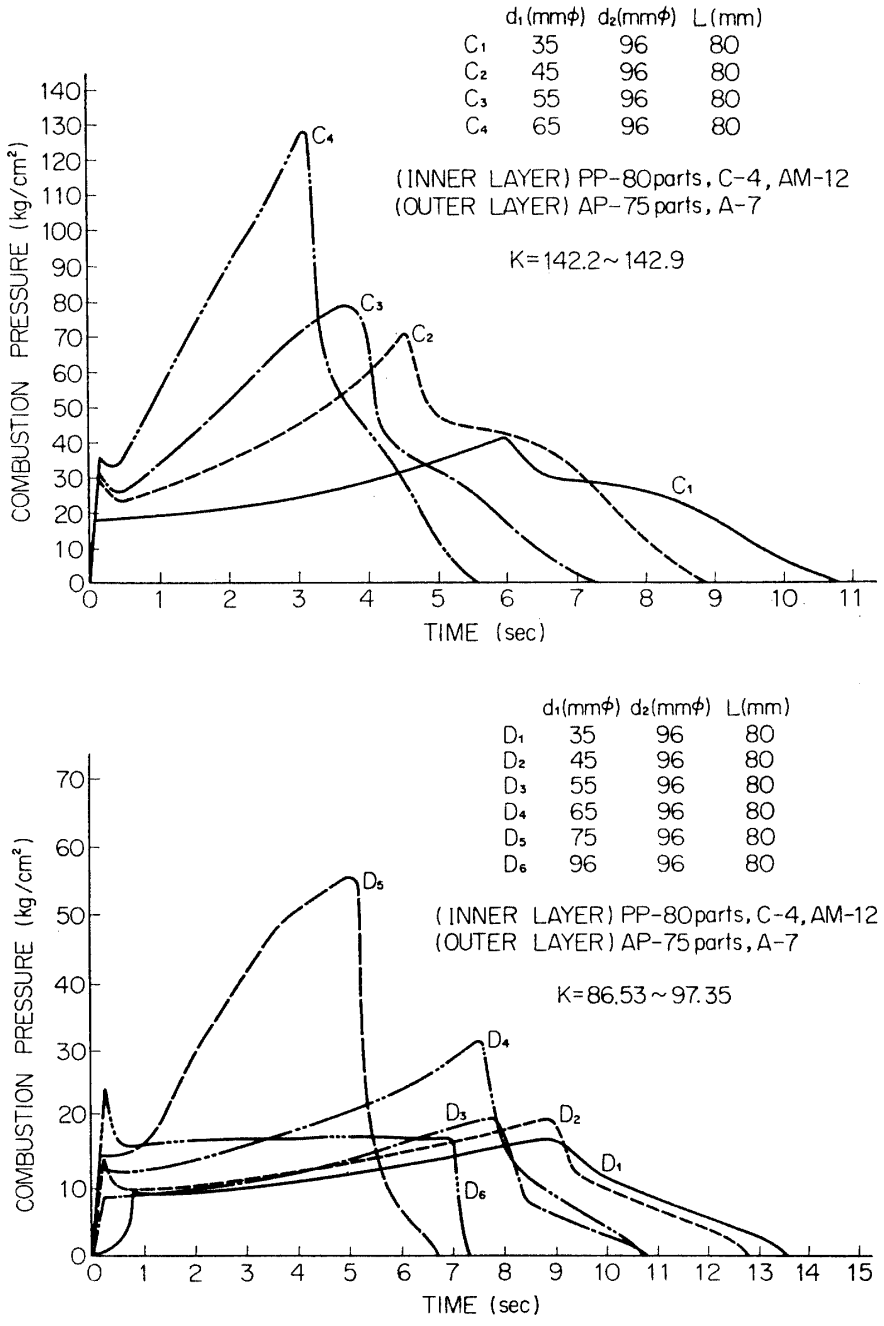

FIG. 3. Pressure-time histories of dual-layer grain.

enced except the case of too thin outer-layer. Performance improvement realized by the dual-layer type may account for 20~30% in the total impulse comparing with the simple end-burning motor utilizing the similar composition to the inner-layer (A).

Another merit obtained by this grain charge method is that a part of the outer-layer remained during the course of the reaction time, becomes a structure member receiving the chamber pressure like with an inside-burning grain motor, and protects the lateral surface of the grain from the bonding separation with linear or restrictor being followed by side-burning transition.

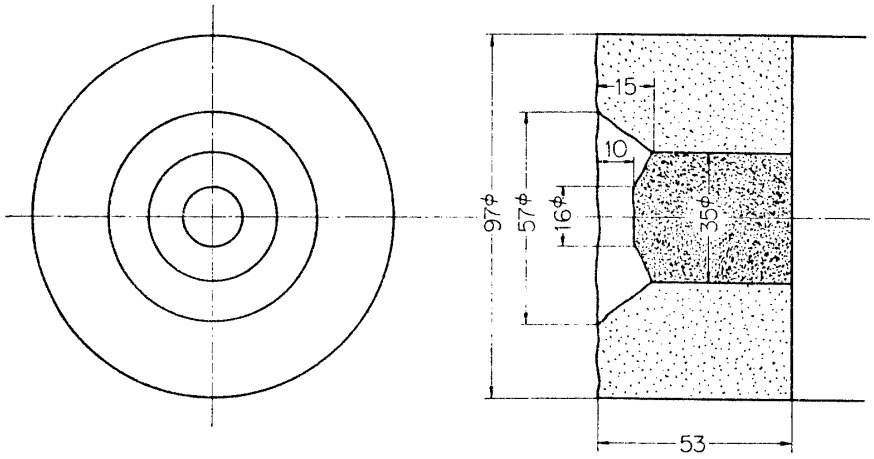

FIG. 4. Contour of grain interrupted steady-state combustion.

An interesting phenomenon is that the progressive pressure-time history is on somewhat higher level than the curves obtained on the basis of the numerical calculation. To explain the reason, inspection was made on the burning surface where its steady-state combustion was interrupted, by means of abrupt destruction of the motor case on the half-way of the firing. A contour of the grain remainder is demonstrated in Fig. 4. The higher regression rate in a gutter part is recognized at the location corresponding to the boundary line on the burning surface. The boundary of two layers situates at its bottom. Thus, increment of the apparent burning surface area naturally makes the slope of the pressure-time curve steeper. It seems that this aspect is brought by an erosive burning; burned gases from one propellant tend to flow parallel or tangentially with respect to the burning surface of another. Turbulence in the vicinity of the impingement of two streams, should induce the higher regression rate at that place, due to the increase in heat feedback transferred

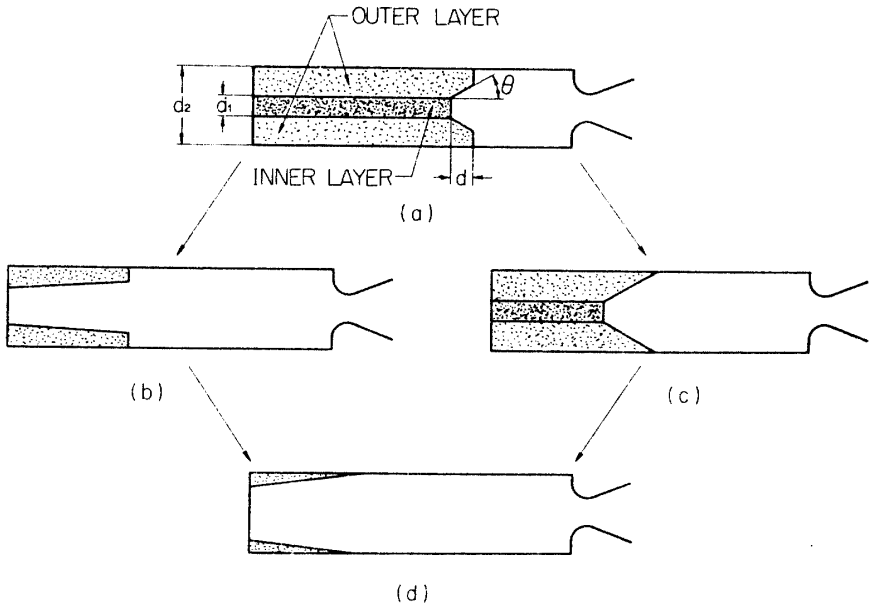

FIG. 5. Predicted variations of the burning surface configuration of the grains.

from the flame zone to the solid surface.

Without such a boundary effect between polyurethane and polybutadiene grain layer, one might predict the variation of a burning surface configuration which seems to pursue in the order of (a)→(b)→(d) or (a)→(c)→(d), as shown in Fig. 5. Thereby, it could state approximately the equation for expressing the burning area of the propellant grain as a function of time. If $r_2/r_1=\sin\theta$ holds, at each burning surface geometry corresponding to the reaction period, the following equations giving the relation between burning area and time can be written:

Region (a)

$$S=\pi\left\{2R_1\left(\frac{1-\sin\theta}{\cos\theta}\right)+\left(\frac{1-\sin\theta}{\cos^2\theta}\right)\right\}\int_0^t(r_1-r_2)dt+\pi R_2^2 \tag{2}$$

at $0<t<t_1$, where R is propellant grain radius, t is a reaction time starting from the instant of the ignition, θ is the angle between the motor axis and the generating line of the burning surface in the form of a trancated cone, and S is the burning surface area. Subscripts 1 and 2 denote the inner and the outer-layer, respectively, t_1 is the minor value of t_k given by either of

$$\int_0^{t_k} r_1dt=L \tag{3-1}$$

or

$$\tan\theta\int_0^{t_k}(r_1-r_2)dt=R_2-R_1 \tag{3-2}$$

where L is the propellant grain length.

Region (b)

When t_1 is determined by Eq. (3-1),

$$S=\frac{\pi}{\cos\theta}\left(L-\int_0^t r_2dt\right)\left\{2\left(R_1+\int_{t_1}^t\frac{r_2}{\cos\theta}dt\right)+\left(L-\int_0^t r_2dt\right)\tan\theta\right\}$$
$$+\pi R_2^2-\pi\left\{R_1+\int_{t_1}^t\frac{r_2}{\cos\theta}dt+\left(L-\int_0^t r_2dt\right)\tan\theta\right\}^2 \tag{4}$$

at $t_1<t<t_2$, where t_2 is given by the following equation;

$$R_2=R_1+\frac{1}{\cos\theta}\int_{t_1}^{t_2} r_2dt+\left(L-\int_0^{t_2} r_2dt\right)\tan\theta \tag{5}$$

Region (c)

$$S=\pi R_1^2+\frac{\pi}{\cos\theta}(R_1+R_2)\left(\int_0^t r_1dt-\int_0^{t_1} r_2dt-\sin\theta\int_{t_1}^t r_2dt\right) \tag{6}$$

at $t<t_1<t_2$, where t_1 and t_2 are determined by Eqs. (3-2) and (3-1), respectively.

Region (d)

$$S=\frac{\pi}{\cos\theta}\left(L-\int_0^{t_m} r_2dt-\sin\theta\int_{t_m}^t r_2dt\right)\left(R_1+R_2+\int_{t_n}^t\frac{r_2}{\cos\theta}dt\right) \tag{7}$$

at $t>t_2$. Terms with $m=2$, $n=1$ describe the case of (a)→(b)→(d) and those with $m=1$, $n=2$ represent the case of (a)→(c)→(d).

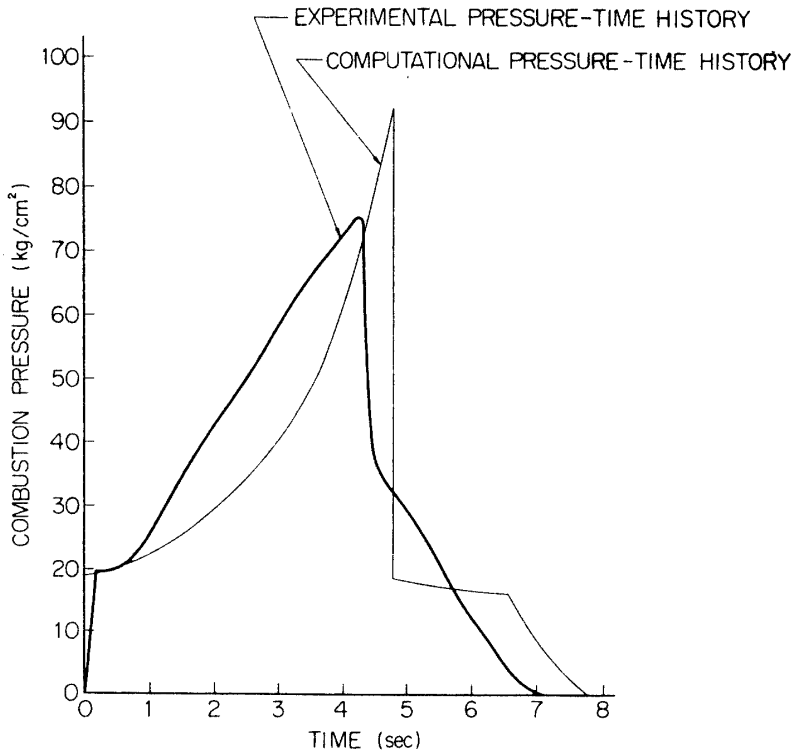

FIG. 6. Comparison of the calculated pressure-time history of the dual-layer grain on the basis of the performance data of the dual-thrust type grain with the actual pressure-time history.

Using above equations and linear burning rate data given in Fig. 2, combustion pressure-time history was derived numerically and compared with the experimental result, as shown in Fig. 6.

Here, the information on the relationship between burning area ratio of two propellants and combustion pressure with a parameter of the restriction ratio, was necessary for the estimation of the pressure-time history of this dual-layer propellant grain motor. For this purpose, initial combustion pressure data obtained by a series of the dual-thrust motor firings described later is available.

An illustrated pressure-time history represented in Fig. 6 shows considerable difference in the measured and calculated results. It is believed that the discrepancy is mainly due to the existence of the gutter on the burning surface.

2.2. Observation of the Steady-State Combustion by Means of a Transparent Motor

A technique in achieving direct observation of the combustion process is presented for making successive analysis of the ignition phenomena, burned gas behavior, burning surface configuration through the reaction time. Up to the present, photographic observation has been made by several investigators [*3*] [*4*] using transparent windows on the head end of the rocket motors. These observations showed very little of the combustion zone and gas stream inside the chamber because of smoke, window itself and so on. One-dimentional chamber whose

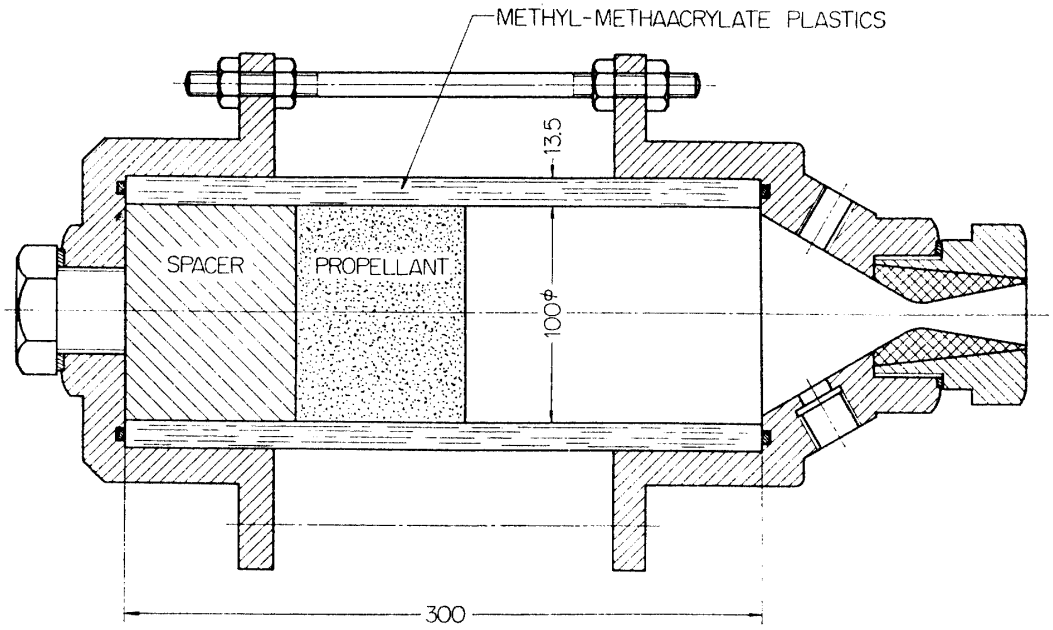

FIG. 7. Drawing of one-dimentional transparent motor.

cylindrical portion is all made of transparent material, is free from wall hazing during reaction time and provides available photograph for the study of the unstable combustion.

Fig. 7 shows a transparent end-burning rocket motor used in this study. The cylindrical portion of the motor is made of polymethylmethaacrylate plastic of 13.5 mm in thickness and 100 mm in inner diameter. Firing experiments have been conducted up to the combustion pressure of 45 kg/cm^2, using this motor.

The local gas velocity, homogeneity of the burned products containing condensed particles and burning surface regression rate may be measured directly, except in the portion covered by metallic hardware of fore-head and nozzle, and the restricted part on the lateral surface of the grains.

As the tools for studying the combustion process inside the chamber 16 mm high speed motion picture, 8 mm color motion picture and 35 mm frame motor-driving cameras were employed. Illustrated photographs for dual-layer propellant grain combustion compared with simple end-burning are shown in Fig. 8. At any case, emissive and dense clouds can be noted in the vicinity of the burning surface. They seem to be what metal or metal oxide ingredients are radiating. From each trace of the incandescent particles, it has been found that they are accelerated somewhat toward the nozzle direction. In the case of the simple end-burning, particle velocity attains to a steady-state at the downstream of 2~5 cm from the burning surface. This distance might correspondingly predict burning life time of "Magnarium" particles, though there are some questions as to whether the luminous particle velocity is consistent with that of the main gas flow.

Some investigations on Al-Mg alloy particles carried out by Fassel [5], Wood [6], et al., indicate that the ignitability and the burning rate are consistently higher than those of aluminium particles. From the observation of the burned gas

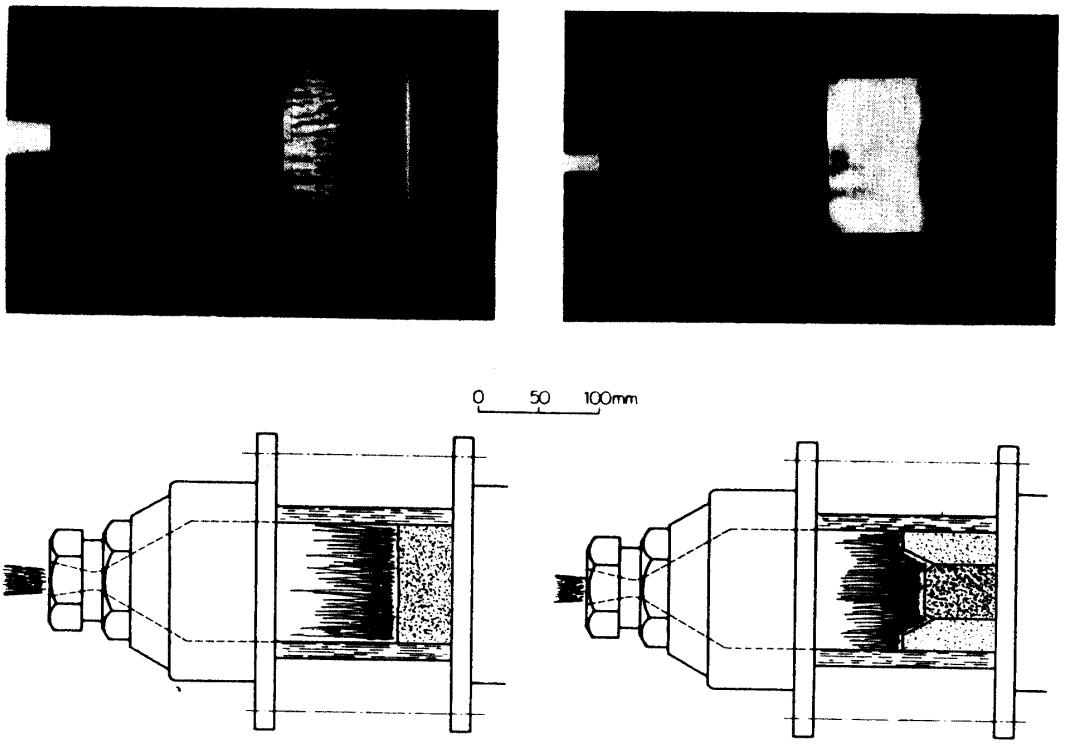

(A) Simple end-burning grain motor
Grain diameter 96 mm
Burning pressure 14.8 kg/cm²

(B) Dual-layer grain motor
Inner-layer grain diameter 55 mm
Outer-layer grain diameter 96 mm
Burning pressure 18.0 kg/cm²

FIG. 8. High speed (500 frames/sec) cinephotographs of steady-state combustion of dual-layer and simple end-burning grains, loaded in the one-dimentional transparent midget motor.

flow in the chamber, it is believed that "Magnarium" particles have completely burned within 40 ms.

Downstream near the nozzle, magnesium oxide condensation can be seen to occur already. Considering that the adiabatic combustion temperature of the inner-layer and the outer-layer are 2,600 and 2,950°K, respectively and on the other hand, the melting points of MgO and Al_2O_3 are 3,173 and 2,303°K, respectively, then there will be no question of whether the condensed particles are mostly magnesium oxide or not, within the limit of the cylindrical chamber. The stream generating from both of inner and outer-layer burning surface perpendicular to the motor axis contains weak turbulence, but in the flow arising from the boundary of these two layers can be recognized intense turbulence. Depicted here are the outmost boundary layer and the gaseous zone of decomposed methylmethaacrylate plastic, and a mixing zone of the reaction product gases of different layers which is located between the concentric flame zones.

Contrast to the dual-layer propellant grain motor, the gas flow inside the simple end-burning propellant grain motor is of less turbulence on the similar combustion pressure level, where Reynolds number of the flow is roughly estimated to be 30,000~40,000. Accordingly, at any case the gas flow in the chamber should be in the turbulent region. Emissive clouds observable in the simple end-burning

grain are of a cellular form with a vapor trail, whereas in the dual-layer grain, the droplet envelopes are difficult to be discriminated due to the intense turbulence until they reach at a distance from the burning surface.

2.3. Application of Dual-Layer Propellants to Dual-Thrust Type Motor

Static firing tests

Progressive thrust generation can be obtained by using dual-layer grain of the end-burning type. However, these will not give the vehicle initial thrust and manouvering speed enough to launch them with sufficient acceleration. Therefore, there is real need for simple and expensive means increasing the impulse during the ignition period in the end-burning motor. Design utilizing the end-burning and radial-burning grain combination, at the fore-head and aft-end sides, respectively, delivers two thrust stages. It develops a high level of thrust for a short period of the reaction time during the booster stage, then follows a lower level of thrust for a long time with the end-burning.

A dual-thrust grain combining the dual-layer with the radial-burning propellant as shown in Fig. 9, is made to cover the undesirable nature inherent to the end-burning grains. Hence an advantage of such a dual-thrust type is that the radial-burning portion remained at a sustainer stage protects the chamber wall from being exposed to flame during the greater part of the reaction time.

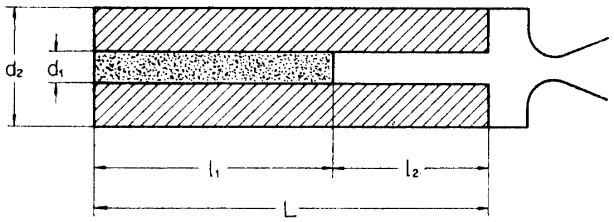

Fig. 9. Schematic drawing of dual-thrust type grain.

As shown in Fig. 10, the pressure-time history resembles to that of the dual-layer grain burning, but a magnitude of the initial thrust increased, resulting in an improved launching capability. Unstable combustion attributed to an acoustic oscillation has not taken place under the prescribed conditions. As well as with the dual-layer grain, one may obtain a considerable improvement in specific impulse and total thrust owing to the increment of grain loading density and by making possible the motor operation at the higher combustion pressures.

Relation between the initial burning pressure and the initial area fraction of each grain layer at some restriction ratios

In order to estimate a pressure-time history with the dual-layer grain motor, combustion pressure as a function of the relative burning area fractions of these two layers must be determined experimentally. For this purpose, it is essential to know the combustion pressure under the firing condition where erosive burning and boundary effect on the burning surface of the grains are negligible. Dual-

thrust motors herein are appeared to be appropriate for relating the combustion pressure to the burning area fraction of the layers on the basis of the initial pressure.

A cross point of extrapolation lines made of the ignition pressure rise and the steady-pressure portion was defined as an initial combustion pressure. Fig. 11 gives the plots of the initial combustion pressure obtained by a series of the firing tests at different restriction ratios. Numerical estimation on the pressure-time history of the dual-layer grain illustrated in Fig. 6 was made by utilizing Eqs. (1)~(7) and interpolated or extrapolated values of the data in Fig. 11.

On the other hand, initial combustion pressure dependency upon the restriction ratios emerges into the following equation, if the corresponding partial pressure law to the burning area of each propellant grain layer holds in the chamber,

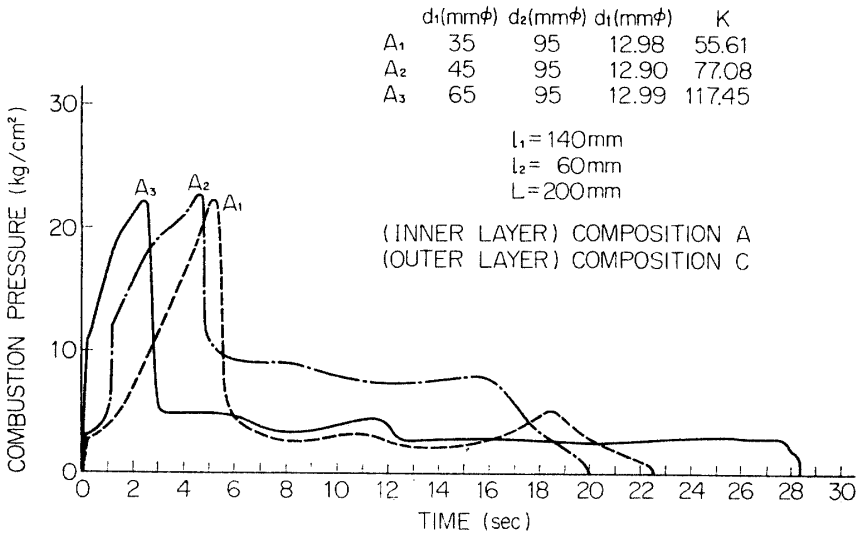

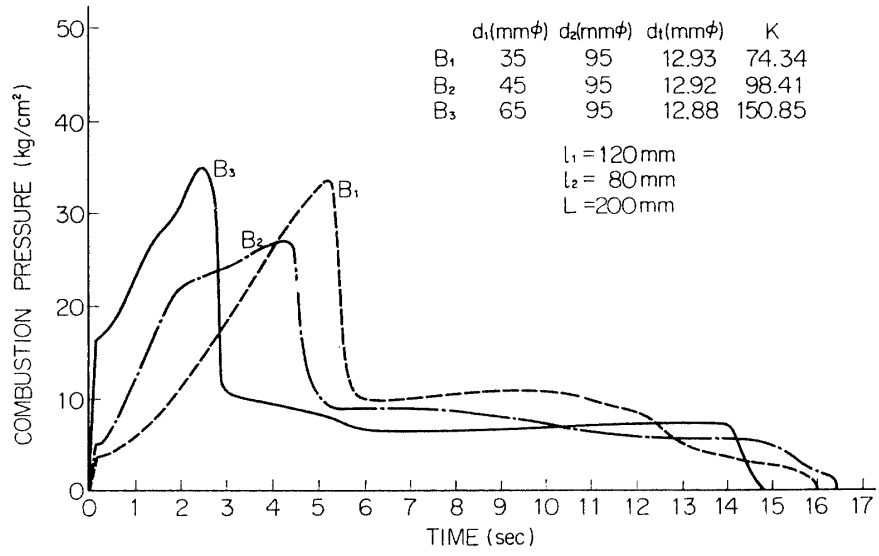

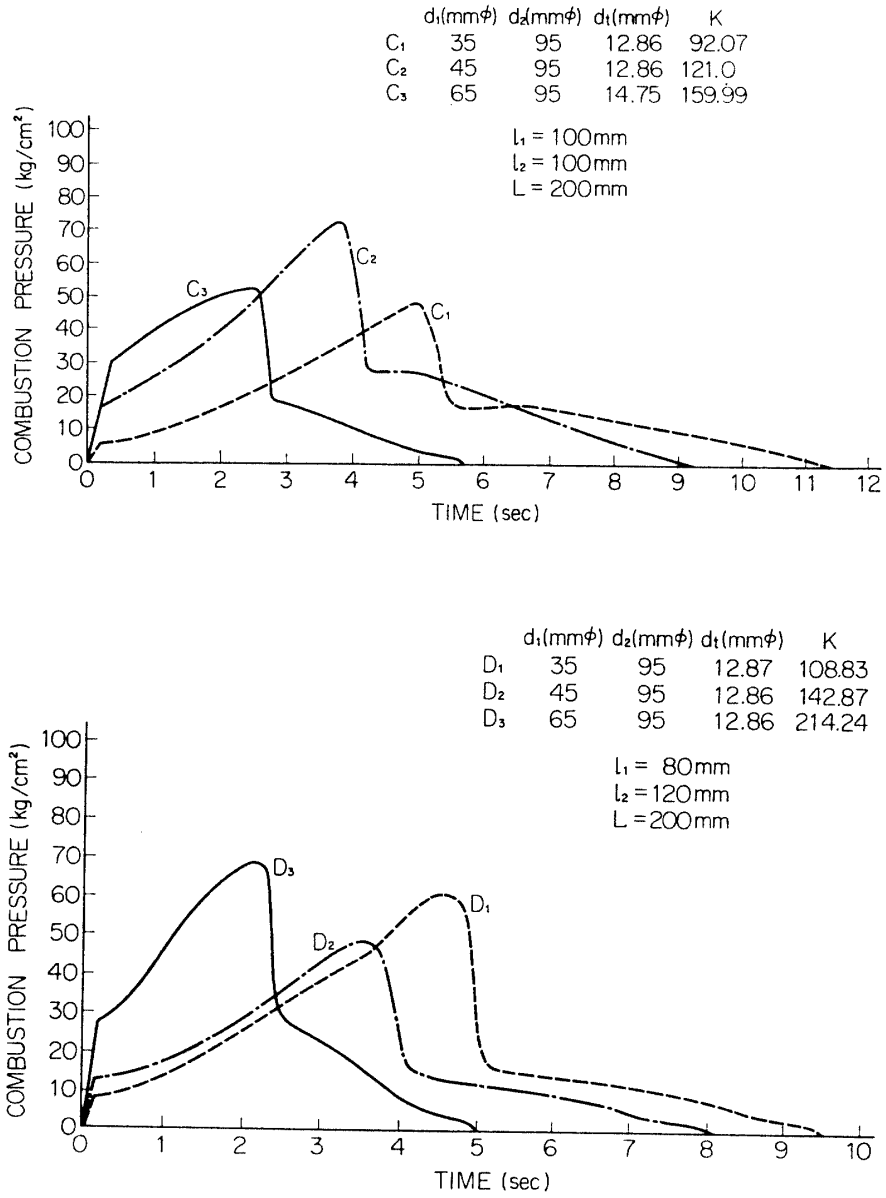

FIG. 10. Pressure-time histories of dual-thrust type grain.

neglecting the variation of the combustion temperature with the combustion pressure:

$$K_0 = \frac{1}{\alpha p_i^{(n_1-1)}(\Delta S_1) + \beta p_i^{(n_2-1)}(\Delta S_2)} \tag{8}$$

where p_i is the initial combustion pressure, K_0 is the initial restriction ratio, ΔS_1 and ΔS_2 are the initial burning area fractions of the inside polybutadiene propellant and the outside polyurethane propellant layer, respectively. α and β are constants. It would be difficult to derive the accurate values for these constants theoretically, but a number of tests are still possible to determine them from the fit of the firing data. Solid lines through the points drawn in Fig. 11 may be represented by the

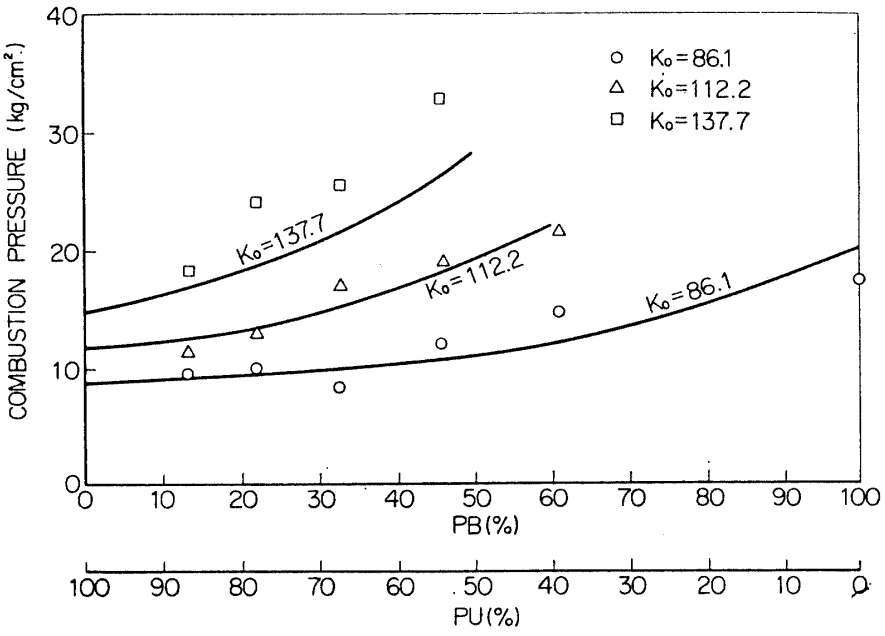

FIE. 11. Relation between burning surface area percentage and combustion pressure (Solid lines are drawn based on Eq. (9)).

following equation for inside (A) and outside-layer (C):

$$K_0=\frac{1}{2.96(10^{-4})p_i^{-0.31}(\Delta S_1)+8.11(10^{-4})p_i^{-0.9}(\Delta S_2)} \tag{9}$$

Although the above equation is in considerable deviation from the experimental values, it can be said that this prediction for the chamber pressure given as a summation of the partial pressure corresponding to each initial burning surface area of polyurethane and polybutadiene grains should be valid if not erosive burning.

3. Concluding Remarks

With a dual-layer propellant grain the higher average combustion pressure may be achieved and fair improvement in the ballistic performance will be expected.

There are optimum design parameters for both dual-layer and dual-thrust type motor. For instance, when L/D ratio of the dual-layer grain is 0.83, available ratio of the inner to the outer-layer is 0.4~0.7. However, as L/D ratio of the grain increases, the upper limit of this ratio decreases.

The progressive nature of the pressure-time history is characterized by becoming steeper than the predicted result numerically.

Inspection made on the burning surface where the steady-state combustion was interrupted, clarified that at the grain layer boundary there was a circular gutter. At this place the regression rate is substantially higher than at any other point, and such an effect that numerically predicted pressure-time history does not account for, will contribute to the gradient increase. This phenomenon attributes probably to a mechanism included in an erosive burning.

It was observed by means of a transparent motor that the combustion gas flow was of more intense turbulence with the dual-layer grain than with the simple end-burning grain, although even in the latter, the gas flow was in the turbulent region.

Magnesium oxide condensation occurred already in the cylindrical portion of a motor near the nozzle inlet and distinguished the core stream of burned gas of polybutadiene grain layer from the outside burned gas flow of polyurethane grain with a turbulent mixing zone between them.

By application of the dual-layer grain to dual-thrust type motor, a suitable initial thrust will be given. The initial pressure data suggests that the partial pressure law corresponding to each burning area of two layers would approximately hold in these types of dual-thrust grain combining dual-layer with radial-burning propellant grain under the condition of no erosive burning.

Propellant Division
Department of Materials
Institute of Space and Aeronautical Science
University of Tokyo.
October 3, 1966

References

[1] Barrère, M. and Jaumotte, A.: "Rocket Propulsion" (Elsevier Publishing Co., 1960) pp. 343~345.
[2] Barrère, M. and Larue, P.: La Recherche Aéronautique No. 91 pp. 33~41 (1962).
[3] Mathes, H. B., McGie, M. R., Crump, J. E., and Price, E. W.: U.S. Naval Ordance Test Station, Progress Report No. TPR 239 (NOTS 2407), 1960. CONFIDENTAIAL.
[4] Larue, P.: La Recherche Aéronautique No. 91 pp. 23~31 (1962).
[5] Fassel, W. M., Papp, C. A., Hildenbrand, D. L., and Sernka, R. P.: ARS Progress in Astronautics and Rocketry (Academic Press Inc., New York, 1960), Vol. 1, pp. 259~269.
[6] Wood, W. A.: Ibid. Vol. 1, pp. 287~291.